Individual Quantum Probes for Optimal Thermometry

Luis A. Correa,[1,*] Mohammad Mehboudi,[1] Gerardo Adesso,[2] and Anna Sanpera[3,1]

[1]*Departament de Física, Universitat Autònoma de Barcelona - E08193 Bellaterra, Spain*
[2]*School of Mathematical Sciences, The University of Nottingham, University Park, Nottingham NG7 2RD, United Kingdom*
[3]*Institució Catalana de Recerca i Estudis Avançats - E08011 Barcelona, Spain*

The unknown temperature of a sample can be estimated with minimal disturbance by putting it in thermal contact with an individual quantum probe. If the interaction time is sufficiently long so that the probe thermalizes, the temperature can be read-out directly from its steady state. Here we prove that the optimal quantum probe, acting as a thermometer with maximal thermal sensitivity, is an effective two-level atom with a maximally degenerate excited state. When the total interaction time is insufficient to produce full thermalization, we optimize the estimation protocol by breaking it down into sequential stages of probe preparation, thermal contact, and measurement. We observe that frequently interrogated probes initialized in the ground state achieve the best performance. For both fully and partly thermalized thermometers, the sensitivity grows significantly with the number of levels, though optimization over their energy spectrum remains always crucial.

PACS numbers: 05.30.-d, 03.65.Yz, 06.20.-f

Introduction.—With the advent of quantum technologies, the study of the thermodynamics of quantum devices has attracted considerable attention [1,2]. In particular, there is a growing interest in obtaining accurate temperature readings with nanometric spatial resolution [3–5], which would pave the way towards many groundbreaking applications in medicine, biology, or material science. This motivates the development of precise quantum thermometric techniques.

Recent progress in the manipulation of *individual* quantum systems has made it possible to use them as temperature probes, thus minimizing the undesired disturbance on the sample. Fluorescent thermometry may be implemented, for instance, on a single quantum dot to accurately estimate the temperature of fermionic [6,7] and bosonic [8,9] reservoirs. Similarly, the ground state of color centers in nanodiamonds has already been used as a fluorescent thermometer [3–5], achieving precisions down to the millikelvin scale, and a spatial resolution of few hundreds of nanometers. Thermometry applied to micromechanical resonators [10–12] and nuclear spins [13] has also been a subject of investigation. Other studies have focused on more fundamental questions such as the scaling of the precision of temperature estimation with the number of quantum probes [14], and the potential role played by coherence and entanglement in simple thermometric tasks [15].

In this Letter, we investigate the fundamental limitations on temperature estimation with individual quantum probes. Two complementary scenarios are considered. In the first one, we assume that the thermometer reaches thermal equilibrium with the sample. We then determine which are the optimal probes that maximize the attainable precision in the estimation of the temperature. Alternatively, we also consider the situation in which the probe does not thermalize completely due to some constraint on the total estimation time (e.g., the sample may be unstable). In this second scenario, we analyze the dissipative time evolution of the probe in order to optimize the thermometric protocol. We model it as a sequence of steps of preparation, thermal contact, and read-out.

Our main results are the following. First, we show that a N-dimensional equilibrium probe with maximum *heat capacity* is optimal for thermometry. This is an effective two-level probe with $(N-1)$ degeneracy in the excited state at some optimal gap. The maximum achievable precision grows with the dimension of the probe, yet the range of temperatures for which it operates efficiently as a thermometer becomes narrower. In contrast, a less sensitive probe with an equispaced energy spectrum, such as a quantum harmonic oscillator, features wider operation ranges. On the other hand, when the estimation time is limited, we find that a frequently measured probe initialized in its ground state achieves the largest thermal sensitivity. In this case, the overall precision still scales with the dimension of the probe, even though the temperature range for efficient operation is dimension independent.

Our results contribute not only to the theoretical advance of temperature estimation in the quantum regime, but also have potential technological impact for the development of high precision thermometry at the nanoscale.

Fully thermalized thermometers.—In standard thermometry, a (sufficiently small) thermometer is simply allowed to equilibrate with the sample to be probed, so that the temperature of the latter is inferred from the state of the probe. In a quantum scenario, the same procedure can be applied. A first approximation to the sample temperature

can be obtained by performing a suitable measurement on the steady state of the thermalized probe. If a large number ν of such independent experiments is carried out, one can refine the estimate T of the sample temperature. Its corresponding uncertainty ΔT is bounded from below by a geometric quantity $\mathcal{F}(\hat{\varrho}_T)$, known as the quantum Fisher information (QFI) [16], via the quantum Cramér-Rao inequality [17,18]

$$\Delta T \geq [\nu \mathcal{F}(\hat{\varrho}_T)]^{-1/2}. \tag{1}$$

In the present context of temperature estimation, the QFI can be interpreted as the infinitesimal distance, according to the Bures metric, between a thermal state at temperature T, and a thermal state at temperature $T + \delta$ [18]. Intuitively, the more such a distance, the more the initial probe state is sensitive to a small variation of temperature. Formally,

$$\mathcal{F}(\hat{\varrho}_T) = -2\lim_{\delta \to 0} \partial^2 \mathbb{F}(\hat{\varrho}_T, \hat{\varrho}_{T+\delta})/\partial\delta^2, \tag{2}$$

where $\mathbb{F}(\hat{\varrho}_1, \hat{\varrho}_2) \equiv (\mathrm{tr}\sqrt{\sqrt{\hat{\varrho}_1}\hat{\varrho}_2\sqrt{\hat{\varrho}_1}})^2$ is the Uhlmann fidelity between states $\hat{\varrho}_1$ and $\hat{\varrho}_2$, which defines their respective Bures distance via $d_{\mathrm{Bures}}(\hat{\varrho}_1, \hat{\varrho}_2) = 2(1 - \sqrt{\mathbb{F}(\hat{\varrho}_1, \hat{\varrho}_2)})$ [18]. Further to the intuitive meaning of the QFI, we note that there exists an optimal estimator (i.e., an optimal measurement procedure on the final thermalized state) for which the bound in Eq. (1) becomes tight for an asymptotically large number of measurements ($\nu \gg 1$), and can be indeed saturated by means of adaptive metrological schemes [16]. Therefore, the inverse of the QFI equivalently defines the minimum achievable variance in the estimation of T. We will then refer to $\mathcal{F}(\varrho_T)$ as "thermal sensitivity" and consider it as a benchmark for optimality in the following analysis [8–11,14,19].

We write the Hamiltonian of our probe as $\hat{H} = \sum_n \epsilon_n |\epsilon_n\rangle\langle\epsilon_n|$. A thermalization process leads to stationary states of the form $\hat{\varrho}_T = \sum_n p_n |\epsilon_n\rangle\langle\epsilon_n|$, where the populations are $p_n \equiv Z^{-1}e^{-\epsilon_n/k_B T}$ and the partition function is given by $Z \equiv \mathrm{tr}\, e^{-\hat{H}/k_B T}$. In what follows we set $\hbar = k_B = 1$.

In the energy eigenbasis, Eq. (2) rewrites as [20]

$$\mathcal{F}(\hat{\varrho}_T) = 4\sum_{m,n} p_m \frac{|\langle\epsilon_m|\partial_T\hat{\varrho}_T|\epsilon_n\rangle|^2}{(p_m + p_n)^2} = \frac{\Delta\hat{H}^2}{T^4}, \tag{3}$$

were $\Delta\hat{H}^2 \equiv \langle\hat{H}^2\rangle - \langle\hat{H}\rangle^2$. In this last step, we have used the identity $\langle\hat{H}\rangle = T^2\partial_T \ln Z$. Interestingly, in the single shot scenario of $\nu = 1$, one can combine Eqs. (1) and (3) to get the thermodynamic uncertainty relation $(\Delta T/T^2)\Delta\hat{H} \geq 1$. Also, note that $\Delta\hat{H}^2/T^2 = d\langle\hat{H}\rangle/dT \equiv C(T)$ which, in the present case, may be referred to as the "heat capacity" of the probe. It thus follows that the signal-to-noise ratio $T/\Delta T$ is upper bounded as $(T/\Delta T)^2 \leq C(T)$ [21]. Note as well that, since $\hat{\varrho}_T$ is a thermal state, the most informative measurement saturating Eq. (1) is just a projection onto the energy eigenbasis.

In light of Eq. (3), the maximization of the thermal sensitivity of a probe translates into finding the energy

spectrum with the largest possible energy variance at thermal equilibrium, or equivalently, the N-dimensional probe with the largest heat capacity. Note that the heat capacity of the sample must be much larger, anyway, than that of the probe so as to minimize any disturbance arising from the estimation procedure.

For a general N-level probe, the energy variance writes as $\Delta\hat{H}^2 = Z^{-1}\sum_n \epsilon_n^2 e^{-\epsilon_i/T} - (Z^{-1}\sum_n \epsilon_n e^{-\epsilon_n/T})^2$. The variance is bounded. In order to identify its maximum, we impose $\partial_{\epsilon_n}\Delta H^2 = 0$, which results in a set of N transcendental equations. Subtracting the mth equation from the nth one ($\partial_{\epsilon_n}\Delta\hat{H}^2 - \partial_{\epsilon_m}\Delta\hat{H}^2 = 0$), we arrive at the condition $(\epsilon_n - \epsilon_m)[\epsilon_n + \epsilon_m - 2(\langle\hat{H}\rangle + T)] = 0$ (see Ref. [22] for details). That is, any two energy eigenvalues ϵ_n and ϵ_m must be either equal, or sum up to the same value at the stationary points of $\Delta\hat{H}^2$. This may only happen if the energy spectrum is that of an effective two-level atom with energies $\{\epsilon_-, \epsilon_+\}$ and some ground and excited-state degeneracies given by N_0 and $N - N_0$, respectively. Without loss of generality, we may always shift the energy spectrum so that $\epsilon_- = 0$ and the optimal gap becomes $x^*_{N,N_0} \equiv \Omega^*/T = (\epsilon_+ + \epsilon_-)/T = 2(1 + \langle\hat{H}\rangle/T) > 2$, since now $\langle\hat{H}\rangle > 0$. This optimal gap may be conveniently rewritten as $e^{x^*_{N,N_0}} = [(N - N_0)/N_0] \times [(x^*_{N,N_0} + 2)/(x^*_{N,N_0} - 2)]$. Observing that the difference $\Delta\hat{H}^2(x^*_{N,N_0-1}; N, N_0 - 1) - \Delta\hat{H}^2(x^*_{N,N_0}; N, N_0) = \frac{1}{4}(x^{*2}_{N,N_0-1} - x^{*2}_{N,N_0})$ is always positive, one can conclude that the excited-state degeneracy must be the largest possible (i.e., $N_0 = 1$) so as to maximize the energy variance.

Finally, to ensure that $\Delta\hat{H}^2$ reaches a maximum at x^*_{N,N_0}, we must check that the Hessian matrix ($\mathcal{H}_{ij} \equiv \partial^2\Delta\hat{H}^2/\partial\epsilon_i\partial\epsilon_j$) is negative definite in that configuration. After a tedious but otherwise straightforward calculation, we can see that it has $N - 2$ identical eigenvalues $\lambda_1 = -\frac{1}{2}[(x^*_{N,1} - 2)/(N - 1)]$, plus two nondegenerate ones: $\lambda_2 = -\frac{1}{8}[(x^{*2}_{N,1} - 4)/(N - 1)]$ and $\lambda_3 = 0$. Since $x^*_{N,1} > 2$, both λ_1 and λ_2 are negative. The single vanishing eigenvalue λ_3 simply reflects the symmetry of $\Delta\hat{H}^2$ with respect to a global shift of all energy levels. Hence, one may rigorously conclude that the effective two-level configuration described above indeed maximizes the energy variance. See Ref. [23] for an alternative derivation.

Here is the final expression for the corresponding QFI:

$$\mathcal{F}_N = \frac{x^4 e^x}{\Omega^2}\frac{N - 1}{(N - 1 + e^x)^2}, \tag{4}$$

which is indeed maximal at $x = x^*_{N,1}$. In Fig. 1, we plot Eq. (4) for different values of N. The precision in temperature estimation improves significantly by increasing the dimensionality N of the probe, albeit at the expense of reducing the specified temperature range for efficient operation of the probe as a thermometer (see inset of Fig. 1).
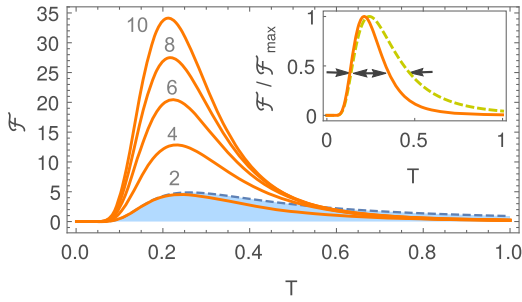
FIG. 1 (color online). QFI versus sample temperature for optimized N-dimensional probes (orange) with $N = \{2, 4, 6, 8, 10\}$. The dashed blue line represents the QFI of a harmonic probe and the shaded blue area is the domain reachable by finite-dimensional probes with an equispaced spectrum. In the inset, the normalized sensitivities of two probes with $N = 2$ (dashed green) and $N = 10$ (solid orange) are compared. The arrows indicate the width of the specified temperature range. Temperature and QFI are both expressed in arbitrary units and $\Omega = 1$.

So far, we have seen that the best thermometers are effective two-level atoms with a highly degenerate excited state and a specific temperature-dependent gap. However, these may be very hard to prepare in practice, especially due to the fact that the sample temperature must be known precisely. For this reason we now consider more versatile suboptimal probes with a richer spectrum, such as a single thermalized harmonic oscillator. In this case, the corresponding QFI can be easily computed from the 2×2 steady-state *covariance matrix* [24,25] of a thermal state $\boldsymbol{\sigma}_T = \coth(\Omega/2T)\mathbb{1}_2$ as in Eq. (2). Using the fact that the Uhlmann fidelity between two single-mode Gaussian states $\boldsymbol{\sigma}_1$ and $\boldsymbol{\sigma}_2$ is given by $\mathbb{F}(\boldsymbol{\sigma}_1, \boldsymbol{\sigma}_2) = 2(\sqrt{\Delta + \Lambda} - \sqrt{\Lambda})^{-1}$ [26], where $\Delta \equiv \det(\boldsymbol{\sigma}_1 + \boldsymbol{\sigma}_2)$ and $\Lambda \equiv \det(\boldsymbol{\sigma}_1 - 1) \times \det(\boldsymbol{\sigma}_2 - 1)$, one arrives at $\mathcal{F}_{\mathrm{ho}} = (\Omega^2/4T^4)\mathrm{csch}^2(\Omega/2T)$. This is represented in Fig. 1 with a dashed blue line. For ease of comparison we take the oscillator frequency Ω to be $\epsilon_+ - \epsilon_-$. As we can see, a harmonic probe features a thermal sensitivity similar to that of a two-level probe. Even if harmonic thermometers are outperformed by most optimized N-level probes, they are endowed with a much broader specified temperature range for efficient operation, making them a choice of practical interest. This can be understood by observing that the thermal sensitivity of a probe with a single energy gap may only peak at one characteristic frequency, while with an equispaced, unbounded spectrum there will always be some transition close to resonance.

Partly thermalized thermometers.—All of the previous analysis holds regardless of the probe-sample interactions or the spectral properties of the sample, as long as thermalization takes place. In practice, however, one may have to read-out the temperature *before* attaining full thermalization. This would be the case, for instance, if the sample was unstable and existed only for times comparable to the dissipation time scale. In this alternative scenario, we ask ourselves about the optimal breakup of the total running time of the estimation procedure (t_s) into sequential stages

of probe preparation, thermal contact (during time Δt), and measurement, so as to optimize the achievable precision in Eq. (1). Note that the number of interrogations is now limited to $\nu = t_s/\Delta t$, so that the figure of merit to be maximized is the ratio $\mathcal{F}(\Delta t)/\Delta t$ [27,28].

Since we must monitor the time evolution of the probe, it is necessary now to specify the sample and its coupling with the thermometer. We shall model the sample as a bosonic heat bath, linearly coupled to an arbitrary probe. The total Hamiltonian writes as $\hat{H}_{\mathrm{tot}} = \hat{H} + \sum_\mu \omega_\mu \hat{b}_\mu^\dagger \hat{b}_\mu + \hat{X} \otimes \sum_\mu g_\mu(\hat{b}_\mu + \hat{b}_\mu^\dagger)$, where $\hat{b}_\mu$ is the annihilation operator of mode ω_μ in the sample. We choose the probe-sample coupling constants to be $g_\mu = (\gamma\omega_\mu)^{1/2}$, implying flat spectral density $J(\omega) \sim \sum_\mu (g_\mu^2/\omega_\mu)\delta(\omega - \omega_\mu) = \gamma$ [29]. This sets the time scale $\tau_D \sim \gamma^{-1}$ over which $\hat{\varrho}(t)$ varies appreciably. Tracing out the sample from the overall unitary dynamics and assuming a thermal state $\hat{\chi}_T$ for it, leads to an effective equation of motion of the Lindblad-Gorini-Kossakovski-Sudashan (LGKS) type [30,31], that follows from $\dot{\hat{\varrho}} = \mathrm{tr}_S(d/dt)\{e^{-i\hat{H}_{\mathrm{tot}}t}\hat{\varrho}(0) \otimes \hat{\chi}_T e^{i\hat{H}_{\mathrm{tot}}t}\}$, after sequentially performing the Born, Markov, and rotating-wave approximations (see Ref. [32] for a detailed derivation). Note that the Born approximation implies that no correlations are ever created between the probe and sample, so the latter remains undisturbed throughout the estimation procedure. Note also that, for consistency with the Markov approximation, the temperature of the sample may be not arbitrarily low, as the thermal fluctuations must remain fast compared with τ_D.

In the interaction picture, the master equation can be cast as

$$\dot{\hat{\varrho}} = \Gamma_{\Omega,T}\left[\hat{A}_\Omega\hat{\varrho}\hat{A}_{-\Omega} - \tfrac{1}{2}\{\hat{A}_{-\Omega}\hat{A}_\Omega, \hat{\varrho}\}_+\right]$$
$$+ e^{-\Omega/T}\Gamma_{\Omega,T}\left[\hat{A}_{-\Omega}\hat{\varrho}\hat{A}_\Omega - \tfrac{1}{2}\{\hat{A}_\Omega\hat{A}_{-\Omega}, \hat{\varrho}\}_+\right], \quad (5)$$

where $\hat{A}_{\pm\Omega}$ stands for the relaxation and excitation operator associated with the decay channel at frequency Ω. These follow from the decomposition of $\hat{X} = \sum_\omega \hat{A}_\omega$ as a sum of eigenoperators of the probe Hamiltonian (i.e., such that $[\hat{H}, \hat{A}_\Omega] = -\Omega\hat{A}_\Omega$). It is easy to show that the thermal state $\hat{\varrho} = Z^{-1}e^{-\hat{H}/T}$ is a fixed point of Eq. (5) and, choosing a suitable coupling operator $\hat{X}$, the open dynamics may also be *ergodic*, thus eventually bringing any initial state to thermal equilibrium [32].

For a two-level thermometer with Hamiltonian $\hat{H} = (\Omega/2)\hat{\sigma}_z$, we can take, for instance, $\hat{X} = \hat{\sigma}_x$ from which $\hat{A}_\Omega = |-\Omega/2\rangle\langle\Omega/2|$, while $\hat{A}_{-\Omega} = \hat{A}_\Omega^\dagger$. Here, $|\pm\Omega/2\rangle$ are the corresponding energy eigenstates. Generalizing to the case of an N-level probe with eigenstates $\{|\epsilon_i\rangle\}$, a coupling term like $\hat{X} = \sum_{i\neq 1}|\epsilon_1\rangle\langle\epsilon_i| + |\epsilon_i\rangle\langle\epsilon_1|$ would also thermalize any preparation, where we have labeled the ground state by $|\epsilon_1\rangle$. The resulting relaxation operators are $\hat{A}_{\epsilon_i - \epsilon_1} = |\epsilon_1\rangle\langle\epsilon_i|$. In particular, to

account for our effective two-level systems with excited-state degeneracy we can take the limit $\epsilon_i \to (\Omega/2)$ for $i \neq 1$ and set $\epsilon_1 = -(\Omega/2)$ to get the desired thermalization process. Let us finally comment on the decay rates $\Gamma_{\Omega,T}$, which follow from the power spectrum of the bath correlation function $\langle \hat{S}(t)\hat{S}(0)\rangle_T \equiv \mathrm{tr}\{\hat{S}(t)\hat{S}(0)\hat{\chi}_T\}$, where $\hat{S} \equiv \sum_\mu g_\mu(\hat{b}_\mu + \hat{b}_\mu^\dagger)$. In the specific case of a quantum probe coupled through dipole interaction to the quantized electromagnetic field in three dimensions, one obtains $\Gamma_{\Omega,T} = \gamma\Omega^3(1 - e^{-\Omega/T})^{-1}$ [32].

The problem boils down to solving Eq. (5), transforming the time-evolved state $\hat{\varrho}(t)$ back into the Schrödinger picture (i.e. $\hat{\varrho} \mapsto e^{-i\hat{H}t}\hat{\varrho}e^{i\hat{H}t}$), and computing the QFI according to Eq. (2) [27,33–36]. Note that besides comparing the performance of different types of probes, we must now optimize over their initial state too. We start by considering the simplest case of two-level thermometers. Extensive numerical analysis over different initial states shows that ground-state preparations display maximal thermal sensitivity. This indicates that the presence of initial quantum coherence does not provide any significant advantage for thermometry in this setting.

Thus, by choosing $\hat{\varrho}(0) = |-\Omega/2\rangle\langle-\Omega/2|$ we can combine Eqs. (5) and (3) to compute $\mathcal{F}_2(\Delta t)$ as a function of the interrogation time Δt, starting from a ground state preparation:

$$\mathcal{F}_2(\Delta t) = \frac{x^2[e^x(e^{\Delta t/\tau} - 1) + (1 + e^x)\frac{\Delta t}{2\tau}\operatorname{csch}\frac{x}{2}]^2}{(1 + e^x)^2(e^{\Delta t/\tau} - 1)(1 + e^x e^{\Delta t/\tau})T^2}, \quad (6)$$

where $\tau^{-1} \equiv \gamma\Omega^3 \coth(x/2)$. Equation (6) shows that the details of the thermal fluctuations of the sample, encoded in $\Gamma_{\Omega,T}$, only enter into the dynamics through the scaling factor τ. Hence, even if our choice of a flat spectral density might seem pretty restrictive at first, changing the probe-sample coupling would just amount to a suitable rescaling of time.

In Fig. 2 we plot $\mathcal{F}_2(\Delta t)/\Delta t$ for different preparations. As we can see, the sensitivity of a cold thermal probe peaks at some optimal readout time, after which it must be quickly cooled down to start over another relaxation stage in the estimation protocol. In the limiting case of a ground-state preparation, the overall maximum sensitivity is approached as $\Delta t \to 0$.

Equation (6) can be generalized to any of our highly degenerate effective two-level probes prepared in the ground state. As before, their maximum precision follows from the limit

$$\lim_{\Delta t \to 0} \frac{\mathcal{F}_N(\Delta t)}{\Delta t} = \frac{\gamma T(N-1)x^5 e^{2x}}{(e^x - 1)^3}. \quad (7)$$

We now search for the optimal frequency-to-temperature ratio $\tilde{x}$ that sets an ultimate upper bound on the thermal sensitivity in Eq. (7). This can be expressed implicitly as $e^{\tilde{x}} = (5 + 2\tilde{x})/(5 - \tilde{x})$, which is independent of N. Interestingly, the specified temperature range for efficient operation does not scale with N, at variance with the fully thermalized case.
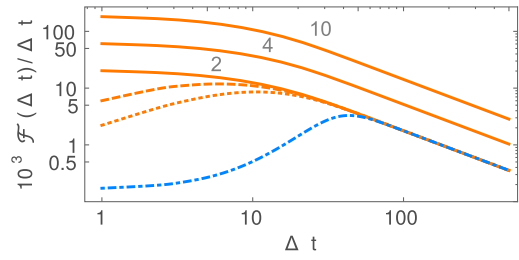

FIG. 2 (color online).   Log-log plot of $\mathcal{F}/\Delta t$ as a function of Δt for different preparations and probe dimensionalities. The continuous orange lines stand for $\mathcal{F}_N$ for probes with $N = \{2, 4, 10\}$ initialized in the ground state. The dashed and dotted orange curves stand for a two-level probe initialized in a thermal state at temperature 0.8 and 0.9, respectively. The dot-dashed blue curve corresponds to a two-level probe prepared in the maximally coherent state $\hat{\varrho}(0) = |+\rangle\langle+|$ ($\Omega/T = \tilde{x}$, $\gamma = 10^{-3}$, and $T = 1$, in arbitrary units).

For completeness, we examine again here the performance of harmonic probes. Going back to Eq. (5), we will set $\hat{H} = \Omega\hat{a}^\dagger\hat{a}$ and $\hat{X} = \hat{a} + \hat{a}^\dagger$, whose corresponding relaxation and excitation operators are trivially $\hat{A}_\Omega = \hat{a}$ and $\hat{A}_{-\Omega} = \hat{a}^\dagger$. The total Hamiltonian is thus quadratic in positions and momenta and therefore, any Gaussian preparation will preserve its Gaussianity in time [24]. Provided that the initial state also has vanishing first order moments ($\langle\hat{x}\rangle = \langle\hat{p}\rangle = 0$), its covariance matrix $\boldsymbol{\sigma}(t)$ alone will be enough for a full description.

In this case, the dynamics may be obtained by explicitly solving the quantum master equation in phase space, to yield $\boldsymbol{\sigma}(t) = e^{-\Gamma_{\Omega,T}t}\boldsymbol{\sigma}(0) + (1 - e^{-\Gamma_{\Omega,T}t})\boldsymbol{\sigma}_T$ [24,37]. Computing the transient QFI is thus straightforward by resorting to Eq. (2). In what follows, we shall consider general (undisplaced) single-mode Gaussian states as initial preparations; these can be written as rotated, squeezed thermal states [24,25]. As it could be expected, ground-state initialization ($\hat{\varrho}(0) = |0\rangle\langle0|$) provides once again the largest thermal sensitivity. One can ignore the temperature dependence of $\Gamma_{\Omega,T}$ in the solution to the master equation and still get a good approximation to $\lim_{\Delta t \to 0}\mathcal{F}_{\mathrm{ho}}(\Delta t)/\Delta t$. Surprisingly, we recover Eq. (7) with $N = 2$. Indeed, this equivalence of two-level probes and harmonic thermometers extends generally beyond the limits $\Delta t \to 0$ and $\hat{\varrho}(0) = |0\rangle\langle0|$. Therefore, at variance with the fully thermalized scenario, the specified temperature range of both oscillators and N-level probes in an effective two-level configuration is virtually the same, regardless of N.

Conclusions.—We have analyzed the performance and ultimate limitations of individual quantum probes for precise thermometry on a sample. Our study is based on techniques of parameter estimation [16,18], and makes use of the quantum Fisher information as an indicator of optimal thermal sensitivity.

First, we have considered a general N-dimensional quantum probe that fully thermalizes with the sample. We have linked the quantum Fisher information with the heat capacity of the probe, and proven that the best

PHYSICAL REVIEW LETTERS

quantum thermometer is an effective two-level atom with a maximally degenerate excited state at a specific energy gap, depending nontrivially on the sample temperature. There exists a complementary trade-off between the maximum achievable estimation precision, which grows with N, and the specified temperature range in which the estimation is efficient, which shrinks with N.

We have also considered the scenario in which, e.g., due to the short lifetime of the sample, full thermalization may not take place. Frequently interrogated probes prepared in their ground state then provide the largest thermal sensitivity. While the maximum achievable precision scales again with N, the specified temperature range is dimension-independent in this case. These results were obtained by considering a large bosonic sample in thermal equilibrium, weakly coupled to the probe through a linear interaction term, ensuring ergodicity. It would be interesting to discuss to what extent can the estimation precision be enhanced with a suitably engineered thermal coupling, e.g., by externally controlling the scattering length in a cold atomic gas [38]. In principle, this would allow the experimenter to directly manipulate the scaling factor τ in Eq. (6).

Finally, it is worth mentioning that even though quantum coherence in the initial state of the probe may not be directly linked to the overall maximization of the precision, the potential role played by *quantumness* in thermometry remains an open problem [13,15] that deserves a study on its own.

---

[*]LuisAlberto.Correa@uab.cat

[1] R. Kosloff, Entropy **15**, 2100 (2013).

[2] R. Kosloff and A. Levy, Annu. Rev. Phys. Chem. **65**, 365 (2014).

[3] P. Neumann *et al.*, Nano Lett. **13**, 2738 (2013).

[4] G. Kucsko, P. Maurer, N. Yao, M. Kubo, H. Noh, P. Lo, H. Park, and M. Lukin, Nature (London) **500**, 54 (2013).

[5] D. M. Toyli, F. Charles, D. J. Christle, V. V. Dobrovitski, and D. D. Awschalom, Proc. Natl. Acad. Sci. U.S.A. **110**, 8417 (2013).

[6] F. Seilmeier, M. Hauck, E. Schubert, G. J. Schinner, S. E. Beavan, and A. Högele, Phys. Rev. Applied **2**, 024002 (2014).

[7] F. Haupt, A. Imamoglu, and M. Kroner, Phys. Rev. Applied **2**, 024001 (2014).

[8] C. Sabín, A. White, L. Hackermuller, and I. Fuentes, Sci. Rep. **4**, 6436 (2014).

[9] U. Marzolino and D. Braun, Phys. Rev. A **88**, 063609 (2013).

[10] M. Brunelli, S. Olivares, and M. G. A. Paris, Phys. Rev. A **84**, 032105 (2011).

[11] M. Brunelli, S. Olivares, M. Paternostro, and M. G. A. Paris, Phys. Rev. A **86**, 012125 (2012).

[12] K. D. B. Higgins, B. W. Lovett, and E. M. Gauger, Phys. Rev. B **88**, 155409 (2013).

[13] C. Raitz, A. Souza, R. Auccaise, R. Sarthour, and I. Oliveira, Quantum Inf. Process. **14**, 37 (2014).

[14] T. M. Stace, Phys. Rev. A **82**, 011611 (2010).

[15] S. Jevtic, D. Newman, T. Rudolph, and T. M. Stace, Phys. Rev. A **91**, 012331 (2015).

[16] V. Giovannetti, S. Lloyd, and L. Maccone, Nat. Photonics **5**, 222 (2011).

[17] H. Cramér, *Mathematical Methods of Statistics* (Princeton University Press, Princeton, NJ, 1999), Vol. 9.

[18] S. L. Braunstein and C. M. Caves, Phys. Rev. Lett. **72**, 3439 (1994).

[19] A. Monras and F. Illuminati, Phys. Rev. A **83**, 012315 (2011).

[20] L. Jing, J. Xiao-Xing, Z. Wei, and W. Xiao-Guang, Commun. Theor. Phys. **61**, 115 (2014).

[21] T. Jahnke, S. Lanéry, and G. Mahler, Phys. Rev. E **83**, 011109 (2011).

[22] See Supplemental Material at http://link.aps.org/supplemental/10.1103/PhysRevLett.114.220405 for further details.

[23] D. Reeb and M. M. Wolf, IEEE Trans. Inf. Theory **61**, 1458 (2015).

[24] A. Ferraro, S. Olivares, and M. Paris, *Gaussian States in Continuous Variable Quantum Information* (Bibliopolis, Napoli, 2005).

[25] G. Adesso, S. Ragy, and A. R. Lee, Open Syst. Inf. Dyn. **21**, 1440001 (2014).

[26] H. Scutaru, J. Phys. A **31**, 3659 (1998).

[27] S. F. Huelga, C. Macchiavello, T. Pellizzari, A. K. Ekert, M. B. Plenio, and J. I. Cirac, Phys. Rev. Lett. **79**, 3865 (1997).

[28] A. W. Chin, S. F. Huelga, and M. B. Plenio, Phys. Rev. Lett. **109**, 233601 (2012).

[29] U. Weiss, *Quantum Dissipative Systems* (World Scientific Pub Co Inc, Singapore, 2008), Vol. 13.

[30] G. Lindblad, Commun. Math. Phys. **48**, 119 (1976).

[31] V. Gorini, A. Kossakowski, and E. Sudarshan, J. Math. Phys. (N.Y.) **17**, 821 (1976).

[32] H. Breuer and F. Petruccione, *The Theory of Open Quantum Systems* (Oxford University Press, New York, 2002).

[33] B. Escher, R. de Matos Filho, and L. Davidovich, Nat. Phys. **7**, 406 (2011).

[34] R. Demkowicz-Dobrzański, J. Kołodyński, and M. Guţă, Nat. Commun. **3**, 1063 (2012).

[35] S. Alipour, M. Mehboudi, and A. T. Rezakhani, Phys. Rev. Lett. **112**, 120405 (2014).

[36] S. Alipour and A. T. Rezakhani, Phys. Rev. A **91**, 042104 (2015).

[37] M. G. A. Paris, F. Illuminati, A. Serafini, and S. De Siena, Phys. Rev. A **68**, 012314 (2003).

[38] P. Haikka, S. McEndoo, G. De Chiara, G. M. Palma, and S. Maniscalco, Phys. Rev. A **84**, 031602 (2011).